



HAL
open science

A progressive damage simulation algorithm for GFRP composites under cyclic loading. Part II: FE Implementation and model validation

Elias N. Eliopoulos, Theodore P. Philippidis

► **To cite this version:**

Elias N. Eliopoulos, Theodore P. Philippidis. A progressive damage simulation algorithm for GFRP composites under cyclic loading. Part II: FE Implementation and model validation. *Composites Science and Technology*, 2011, 71 (5), pp.750. 10.1016/j.compscitech.2011.01.025 . hal-00730298

HAL Id: hal-00730298

<https://hal.science/hal-00730298>

Submitted on 9 Sep 2012

HAL is a multi-disciplinary open access archive for the deposit and dissemination of scientific research documents, whether they are published or not. The documents may come from teaching and research institutions in France or abroad, or from public or private research centers.

L'archive ouverte pluridisciplinaire **HAL**, est destinée au dépôt et à la diffusion de documents scientifiques de niveau recherche, publiés ou non, émanant des établissements d'enseignement et de recherche français ou étrangers, des laboratoires publics ou privés.

Accepted Manuscript

A progressive damage simulation algorithm for GFRP composites under cyclic loading. Part II: FE Implementation and model validation

Elias N. Eliopoulos, Theodore P. Philippidis

PII: S0266-3538(11)00053-4
DOI: [10.1016/j.compscitech.2011.01.025](https://doi.org/10.1016/j.compscitech.2011.01.025)
Reference: CSTE 4920

To appear in: *Composites Science and Technology*

Received Date: 19 August 2010
Revised Date: 24 January 2011
Accepted Date: 30 January 2011

Please cite this article as: Eliopoulos, E.N., Philippidis, T.P., A progressive damage simulation algorithm for GFRP composites under cyclic loading. Part II: FE Implementation and model validation, *Composites Science and Technology* (2011), doi: [10.1016/j.compscitech.2011.01.025](https://doi.org/10.1016/j.compscitech.2011.01.025)

This is a PDF file of an unedited manuscript that has been accepted for publication. As a service to our customers we are providing this early version of the manuscript. The manuscript will undergo copyediting, typesetting, and review of the resulting proof before it is published in its final form. Please note that during the production process errors may be discovered which could affect the content, and all legal disclaimers that apply to the journal pertain.



A progressive damage simulation algorithm for GFRP composites under cyclic loading.

Part II: FE Implementation and model validation

Elias N. Eliopoulos, Theodore P. Philippidis¹

Department of Mechanical Engineering & Aeronautics, University of Patras

P.O. Box 1401, GR 26504 Panepistimioupolis, Rio, Greece

Abstract

The FE implementation of FADAS, a material constitutive model capable of simulating the mechanical behaviour of GFRP composites under variable amplitude multiaxial cyclic loading, was presented. The discretization of the problem domain by means of FE is necessary for predicting the damage progression in real structures, as failure initiates at the vicinity of a stress concentrator, causing stress redistribution and the gradual spread of damage until the global failure of the structure. The implementation of the stiffness and strength degradation models in the principal material directions of the unidirectional ply was thoroughly discussed. Details were also presented on the FE models developed, the computational effort needed and the definition of final failure considered. Numerical predictions were corroborated satisfactorily by experimental data from constant amplitude uniaxial fatigue of multidirectional Glass/Epoxy laminates under various stress ratios. The validation of predictions included fatigue strength, stiffness degradation and residual static strength after cyclic loading.

Keywords: Polymer-matrix composites (PMCs) (A), Fatigue (B), Damage mechanics (B), Finite element analysis (FEA) (C), Life prediction (D)

1. Introduction

¹ Corresponding author: e-mail: philippidis@mech.upatras.gr, Tel. +30-2610-969450, 997235, Fax: +30-2610-969417

The design of lightweight, efficient structures requires extended use of composite materials and development of damage tolerant procedures for life and strength prediction in the presence of accumulated damage. For this kind of analysis, the effect of local failure and stiffness degradation due to cyclic loading, causing stress redistribution, should be investigated. To this end a FATigue DAMAGE Simulator (FADAS) was developed [1] and was implemented as a material model routine in a commercial FE code. Due to the complicated geometry of a real structure and the existence of multiple confined domains in its volume with different in essence mechanical properties, the analytical stress and strain calculations are impossible and only numerical schemes such as the FE method are fit for the purpose.

There are relatively few works published on the subject, most of them in the last two decades. Perhaps, the most complete work of this type of approach was published by Shokrieh and Lessard [2]-[3]. They have developed a method that could be used as a design tool, predicting life, residual stiffness and strength of a laminate based on ply properties.

Van Paepegem et al. [4]-[9] have developed a stiffness degradation based damage mechanics model, using material properties of a cross ply laminate and not of the unidirectional (UD) ply. So, the model does not predict failure modes of the ply but the macroscopic failure of the cross ply laminate. It includes a number of parameters, fitted by experiments on a specific load case (single side displacement-controlled bending) which obviously depend on the stacking sequence and the load case.

Gagel et al. [10] have presented a method for predicting stiffness degradation of a certain lay-up introducing laws for the crack densities in two specified directions, the

parameters of which depend on the stacking sequence and the loading case. Hochard et al. [11] have presented a first ply failure model i.e. non damage tolerant for a woven ply laminate with limited experimental verification however.

Sihn and Park [12] have presented an integrated design module for predicting strength and life of composite structures. No experimental evidence on the validity of their method was presented. Although this type of approach, based on micromechanics, seems promising for the future, from an engineering point of view, composite material properties are certified at the ply level and thus before a life prediction method based on micromechanics could be used, wide agreement on characterization procedures and test methods for fibres and resins should be sought.

Lian and Yao [13] have proposed a FE based method predicting the fatigue life at a single stress ratio ($R=0$) using randomly assigned material properties and stiffness degradation based strength degradation models. They reported satisfactory agreement of numerical predictions and experimental data, however, tests for the input data and verification tests were all performed for the same stress ratio.

In this paper, the FADAS methodology presented in the first part of this work [1], was implemented in a commercial FE code and validated by extensive comparison with uniaxial constant amplitude experimental data from Glass/Epoxy multidirectional (MD) prismatic coupons at various stress ratios, R .

2. FADAS FE implementation

In an earlier numerical implementation of the non-linear version of FADAS for homogeneous stress fields [14], any load sequence was simulated in small steps, e.g. 40

per cycle. Fatigue calculations, i.e. strength and stiffness degradation due to cyclic loading were performed each time a local min or max of each stress component was detected, for the respective stress component. That version of FADAS was validated by constant (CA) and variable amplitude (VA) fatigue tests and residual static strength tests after CA fatigue. In the present FE implementation the simulation time for each load step is much higher. In fact it is a multiple of the number of integration points of the entire FE model, since all calculations are performed separately for each one of them. An alternative approach was followed when the applied loading was of CA. For the time being and for moderate CPU resources, it is not practical to simulate applications of VA loading with the actual FE version of FADAS. Nevertheless, even external loading of CA generates VA cyclic stress components in each ply due to strength and stiffness degradation driven by cyclic loading and local sudden failures, causing stress redistribution.

While the external load is incrementally applied, the max and min values of each component of stress in each ply are determined. When a cycle of the external load is completed, the corresponding stress ratio R_i , and stress amplitude σ_{ia} for each stress tensor component in the principal coordinate system of the layer can be calculated by:

$$R_i = \frac{\sigma_{i_{min}}}{\sigma_{i_{max}}}, \quad i = 1, 2, 6 \quad (1)$$

$$\sigma_{ia} = \frac{\sigma_{i_{max}} - \sigma_{i_{min}}}{2}, \quad i = 1, 2, 6 \quad (2)$$

For each R_i , the number of cycles to failure, N_i , for the developed stress range is calculated by means of linear interpolation from the CLD corresponding to each stress component.

The obtained N_i is required for the calculation of the cumulative life fraction for each stress component that is used in the stiffness degradation models:

$$\sum \frac{n_i}{N_i} \Big|_{(\lambda+1)} = \sum \frac{n_i}{N_i} \Big|_{(\lambda)} + \frac{\Delta n}{N_i}, \quad i = 1, 2, 6 \quad (3)$$

Indices into parentheses in the above relation, i.e. (λ) , $(\lambda+1)$, denote the external load cycle number that was simulated, hence the term Δn in the second term of the right hand side denoting an arbitrary block of CA cycles defined by the user considered to be of the same mean and range as the simulated one. Then, for VA cyclic stress, which is always the case even for CA external cyclic load, the ratio n/N in the stiffness degradation models of Eq. (4) in [1] has to be replaced by the cumulative life fraction given by Eq. (3) above.

At the present FADAS implementation, this parameter, Δn , was left fixed for programming simplicity. For each case, after several numerical experiments, it was selected as a compromise between accuracy and realistic computational effort to have Δn such as to simulate ca. 10 to 20 full cycles (distant by Δn) in the life span of the coupon. Other researchers have developed more sophisticated models using adaptive values of Δn depending on damage accumulation, e.g. [5].

The values of ply engineering constants E_{2t} and G_{12t} for unloading are calculated by multiplying the respective reloading properties, given by Eq. (2) of [1], with 1.001. As the full cycle of external load is simulated for a limited number of times, this value is known to predict very limited increasing permanent strain values. However, even with this value the resulting strain would be different for another user selected Δn block of cycles number but this is not expected to affect FADAS predictions even for matrix dominated lay-ups, concerning number of cycles to failure, residual strength and

stiffness since all material models and failure conditions are stress rather than strain based. Since no reliable experimental data were available for deriving accurate permanent strain models or implementing existing theoretical models, this was the simplest way to introduce increasing permanent strain due to cyclic loading since permanent strain due to increasing stress level and/or local failure was already included in the routine, Eq. (3) in [1] and post-IFF model respectively.

The calculated number of cycles to failure N_i , $i=1,2,6$ are also used with the strength degradation models. When a cycle of external load is completed, the residual tensile strength in the fibres direction $X_{T_r(\lambda+1)}$ is reduced by using an adapted form for VA cyclic stress of the Broutman & Sahu model [15], only if the maximum stress is positive.

The residual tensile strength in the fibre direction at the $(\lambda+1)$ simulated cycle can be readily proved to be given by:

$$X_{T_r(\lambda+1)} = X_T - (X_T - \sigma_{1max}) \left[\frac{X_T - X_{T_r(\lambda)}}{X_T - \sigma_{1max}} + \frac{\Delta n}{N_1} \right] \quad (4)$$

The first term in the brackets, added in $\Delta n/N_1$, is the ratio of the equivalent number of cycles to N_1 , n_{eq}/N_1 , which in turn is the number of CA cycles at the actual stress level of σ_{1max} that would reduce the static strength down to the value of $X_{T_r(\lambda)}$, see Schaff and Davidson [16].

For the compressive residual strength in the fibres direction, the use of the sudden death model, see e.g. Eq. (6) of [1], might be prohibited (numerical precision problems) for high values of the exponent of the equation due to very small reduction of the strength.

In such cases an alternative formulation based on a modified linear model, Eliopoulos [17], can be used:

$$X_{C_r(\lambda+1)} = X_C - \beta(X_C - |\sigma_{1min}|) \left[\frac{X_C - X_{C_r(\lambda)}}{\beta(X_C - |\sigma_{1min}|)} + \frac{\Delta n}{N_f} \right] \quad (5)$$

The constant β is an arbitrary small positive number, e.g. 10^{-3} , 10^{-6} . Its value is not of importance provided that the term $(1-\beta)X_C$ is greater than the largest $|\sigma_{1min}|$ in the time series and almost equal to X_C . Nevertheless, the values suggested in the above were efficiently used for the verification examples presented in this work. The degradation model is supplemented by the following logical statement:

$$\text{If } X_{C_r(\lambda+1)} \leq (1-\beta)X_C + \beta|\sigma_{1min}| \text{ then } X_{C_r(\lambda+1)} = |\sigma_{1min}| \quad (6)$$

Then, a fibres failure in compression (FF_C) damage mode occurs.

The degradation scheme for the compressive residual strength formed of the two Eq. (5) and (6) has a numerically stable sudden death response. Therefore, under C-C and T-C cyclic loading the compressive strength degradation is calculated by means of Eq. (5) and (6); otherwise it remains unchanged.

Implementation in the routine of the residual strength models for the transverse to the fibres direction and in-plane shear was performed in the same way as for the fibre direction.

3. FE models

The FADAS routine has been successfully integrated in ANSYS commercial code and has been adapted to various element formulations; plane strain, 3D brick and shell. For the validation cases presented in this work, all results were derived using the SHELL181 element [18], governed by the Mindlin-Reissner shell theory. It is a 4-node

layered element with six degrees of freedom at each node. The reduced integration option was selected with 1 integration point location at the area of the element and 3 integration points through the thickness of each layer. Non-linear geometry effects were also included although not of great importance for the cases considered, i.e. axial in-plane loading of prismatic coupons.

The user defined material constitutive model was implemented in a FORTRAN routine [19] which was compiled with ANSYS core code and a new executable ANSYS file was created, reducing the solution time a lot, since calculations of the elastic properties for each successive load step were performed at the same time with the stress-strain calculations and not externally later, e.g. using APDL commands. Static analysis was performed, considered to be valid for low strain rate loading cases. Since all verification test data were at room temperature conditions, as it is also approximately the polymeric system cure of the composites, environmental conditions effects were neglected in the analysis.

Two different FE models were developed because of different coupon geometry and stacking sequences of the specimens tested. The ISO 14129 [± 45]_S specimens were modelled with 1920 elements and 4 layers and the standard OB MD specimens, used in the OPTIMAT BLADES project, with 768 elements and 14 layers. Displacements along x and z axes of all nodes located at the left tab area, Fig. 1, except those at the internal edge AB of the tab were constrained. In addition, the y-displacements of all nodes located on the centreline were also constrained. However, all other nodes of the left tab were left free to move in the y-direction to simulate Poisson contraction of the laminate under the compliant tab material. Axial load in the x-direction was equally shared by all the nodes located on the right tab area except those at the internal edge CD of the tab,

Fig. 1. Nodal displacements of the centreline of the same tab were also constrained in the y- and z-direction.

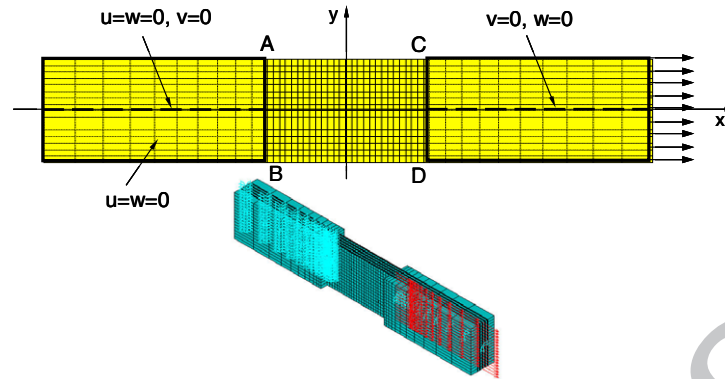


Fig. 1: Boundary conditions shown on OB coupon geometry

4. Computational procedure

An incremental stress-strain analysis was performed and to that end external loading was also applied incrementally. The number of load steps per cycle at different stress ratios was optimized as follows. Under T-C loading ($R=-1$) 60 load steps were foreseen; 40 loading (20 tensile and 20 compressive) and 20 unloading (10 tensile and 10 compressive). Under pure tensile and compressive loadings, $R=0.1$ (T-T) and $R=10$ (C-C) respectively, 30 load steps were realized per cycle; 22 loading and 8 unloading. Upon unloading the material behaviour was assumed linear, so fewer steps were needed. The two load steps after the end of loading or unloading segments are much smaller, e.g. 2 to 3 orders of magnitude less than the other, so as the change of loading condition was detected with negligible stress and strain variation.

For the residual static strength predictions, the FE model was first subjected to CA cyclic loading until the desired life fraction. Then, static loading up to failure was imposed with the load increment being 5 MPa for the $[(\pm 45/0)_4/\pm 45]_T$ model and 1 MPa for that of the $[\pm 45]_s$.

The CPU time needed for each simulation depends of course on the number of elements and layers of the FE model but also on the cycle block number Δn defined by the user. For the MD and the ISO $[\pm 45]_S$ coupons, the CPU time was 6s per load step. Total time for each simulation was a couple of hours in an Intel Core 2 Quad CPU Q6600 @ 2.4 GHz and 4 GB of RAM.

4.1. Final failure

While ply failure in one or more different modes might occur even from the first load steps of the first cycle, depending on the stress level, the routine continues the calculations without interruption until positive definiteness of the laminate stiffness matrix is lost. This might not occur in practice; however, near the final laminate failure a drastic stiffness loss is observed and for this reason the coupon is considered to have failed when the axial displacement of the loaded edge of the model in the loading direction exceeds in a disproportional manner its previous values.

5. Validation of numerical predictions

5.1. Experimental data

The present FE version of FADAS has been implemented with ply properties derived for the OB_UD glass/epoxy composite. For the verification of the numerical predictions, extensive comparison with experimental data was performed. MD laminates made of the basic UD ply material were subjected to various loading conditions consisting of CA cyclic loading of different stress ratios and residual static strength tests after CA loading. All tests were on prismatic specimens under axial loading. All above cited experimental data from MD laminates are not used in FADAS; they are only considered for validating its predictions.

Details on the experimental procedure, measurements and results discussed in this section can be found in the OPTIDAT database and dedicated reports in the OPTIMAT BLADES site [20]-[26].

5.2. Results and discussion

The FADAS routine requires input data only from UD ply material properties, so the entire necessary input set for the FE simulation of any laminate subjected to any loading case was as presented in [1]. The UD ply thickness was set equal to 0.94 mm except for the $+45^\circ$ and -45° layers of the $[(\pm 45/0)_4/\pm 45]_T$ laminate where a thickness of 0.33 mm was used since a bidirectional stitched fabric of ± 45 orientations was used instead of discrete layers from the basic OB_UD composite.

The predicted S-N curves were derived by means of linear regression on a double logarithmic scale of three simulated stress levels for each case. Max and min prediction values presented in the graph results are related to the range Δn of the applied block of cycles, i.e. when failure is predicted at the beginning of a simulated cycle it is not known in which exactly cycle from the Δn has occurred.

FADAS is a general purpose algorithm for multi-axial, VA loading of MD laminates implementing several material models at the principal directions of the UD ply. Any modification of its parameters can potentially affect the results. The performance of all models introduced in accurately representing the average material behaviour is satisfactory, as expected, since all models were fitted to respective UD data by means of non-linear regression. A preliminary sensitivity analysis showed that only the S-N curves definition and constant life diagram formulation, presented in section 4 of [1],

affect drastically the predictions as far as number of cycles to failure, residual strength or stiffness of any MD laminate are concerned.

Simulations were performed for the MD laminated coupons under a great variety of stress ratios, i.e. $R=-0.4$, -2.5 , 0.5 , 0.1 , -1 and 10 and predictions concerning fatigue strength, stiffness and strength degradation were in general satisfactorily corroborated by the test data. Due to space limitations, only few cases are presented in the following sections.

5.2.1. ISO 14129 $[\pm 45]_S$ coupons

Tensile ($R=0.1$) CA loading of the $[\pm 45]_S$ laminate was simulated at three stress levels $\sigma_{\max}=90.6$, 63.6 and 48.5 MPa corresponding to expected number of cycles to failure equal to 1000 , 50000 and $1 \cdot 10^6$ respectively. The predicted numbers of cycles were $450-500$, $37500-40000$, and $900000-950000$ respectively; they were compared with test data reported by Philippidis et al. [20] in Fig. 2. The results are more conservative for the higher stress level and improve at the lower ones.

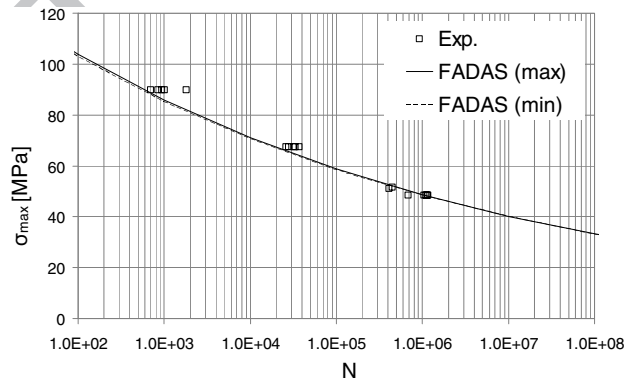


Fig. 2: Comparison between simulation results and exp. data, $[\pm 45]_S$ under $R=0.1$

The predicted axial stiffness degradation of the coupon was compared to the experimental one in Fig. 3. The experimental stiffness was derived by end displacement

data, while the predicted one was determined using the axial displacement of the two most distant nodes on the centreline of the FE model at the edges of the gauge length. The stiffness degradation is predicted to be higher for the lower stress levels following the trend of the experimental data. Nevertheless, simulation results are corroborated by the respective experimental data although more stiff in general.

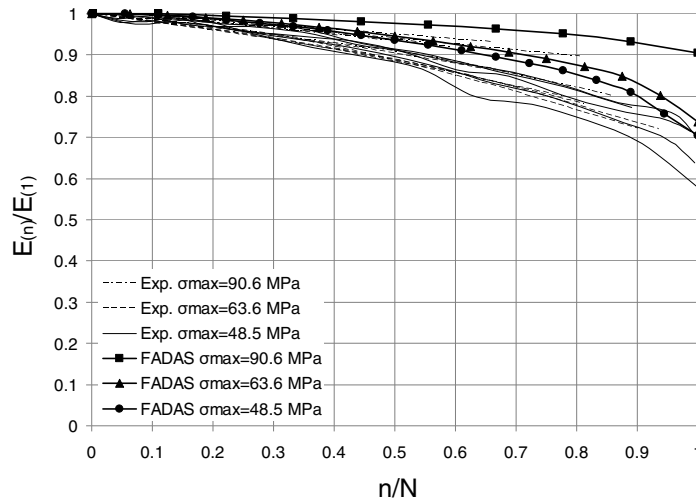


Fig. 3: Validation of stiffness degradation predictions. $[\pm 45]_S$ under $R=0.1$

The residual static strength of ISO 14129 $[\pm 45]_S$ coupons after CA loading up to a certain life fraction was predicted and the results were compared to the respective experimental data (RS exp.) from [23]-[24] and the macroscopic residual strength model of Broutman-Sahu (BR) in Fig. 4. The experimental S-N curve, the static strength (ST exp.) of the intact coupon and the prematurely failed coupons (pr. fail.) during the residual strength test program also appear in the same figure. Tests and simulation were performed at 4 stress levels σ_{max} , namely 78.3 MPa (expected N to failure 5000 cycles), 63.6 MPa (50000 cycles), 55.6 MPa (220000 cycles) and 48.5 MPa ($1 \cdot 10^6$ cycles) for several life fractions, i.e. 0.2, 0.5 and 0.8.

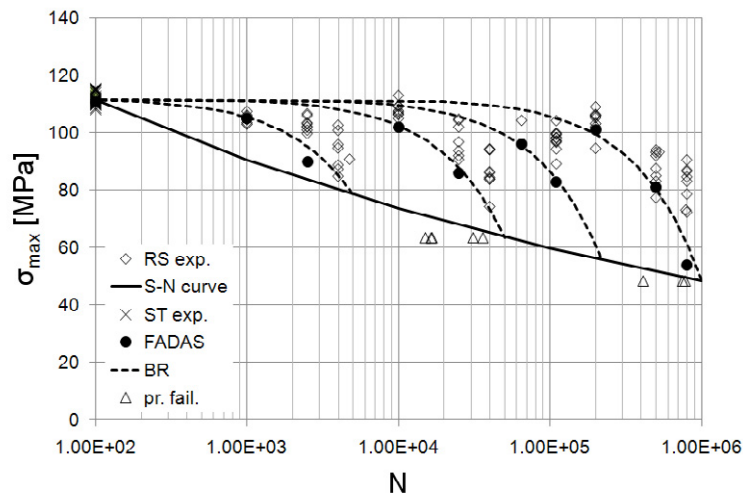


Fig. 4: Residual strength predictions for $[\pm 45]_s$ coupons after CA loading under $R=0.1$

The predictions are in good agreement with the macroscopic residual strength model BR and are corroborated satisfactorily by the experimental data. As also noticed previously, they improve for the lower stress levels. Some numerical results are not displayed because FADAS predicted failure during the CA loading suite.

5.2.2. MD laminate $[(\pm 45/0)_4/\pm 45]_T$ under $R=0.1$

Experimental data for the MD laminate on-axis loaded under various R ratios were reported by Krause and Kensche [21]. Simulation results for the case of T-T ($R=0.1$) CA loading were presented in Fig. 5 along with test data for comparison. Calculations were performed at three stress levels, $\sigma_{\max} = 317, 252$ and 186 MPa with expected number of cycles to failure equal to $5000, 50000$ and $1 \cdot 10^6$ respectively. The corresponding numerical predictions were equal to $N=2000-2250, 27500-30000$ and $600000-650000$.

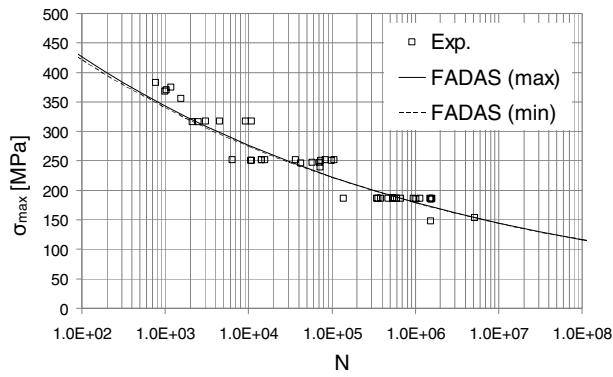


Fig. 5: Comparison of simulation results and test data, $[(\pm 45/0)_4/\pm 45]_T$, $R=0.1$

Concerning stiffness degradation measurements, the strain was measured with an extensometer of 25 mm gauge length for 10 coupons at $R=0.1$; 3 at $\sigma_{\max}=317$ MPa, 4 at $\sigma_{\max}=252$ MPa and 3 at $\sigma_{\max}=186$ MPa [27]. The laminate stiffness was determined by dividing the stress range of each cycle to the respective strain range and was normalized with respect to the stiffness of the first cycle. These data (Exp.) were compared to the respective FADAS predictions (Fig. 6). The predicted stiffness was determined as the slope of the linear regression model of the entire stress-strain loop, with the strain calculated using the axial displacement results from two nodes on the centreline of the FE model distant by 25 mm and was normalized with respect to the stiffness of the first simulated cycle.

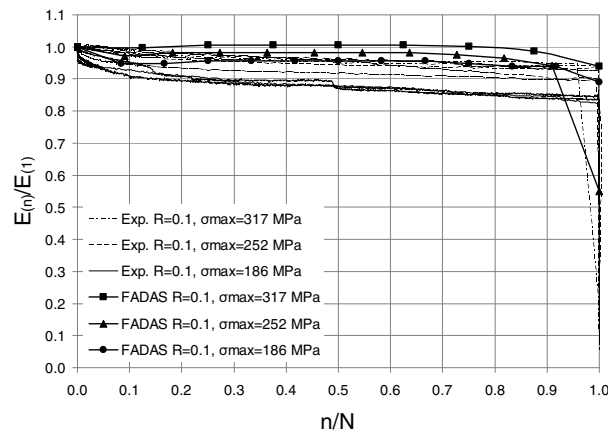


Fig. 6: Validation of stiffness degradation predictions. $[(\pm 45/0)_4/\pm 45]_T$, $R=0.1$

The experimental data show the typical three-stage stiffness degradation of the composite MD laminates reported by several researchers, i.e. rapid stiffness degradation at the beginning of the cyclic loading followed by moderate stiffness degradation for the most of the fatigue life and a drastic stiffness drop near the final failure. It is also observed that the stiffness degradation is higher for the lower stress levels (high-cycle fatigue), which was also observed in other works, e.g. CA fatigue tests on Glass/Polyester MD coupons by Philippidis and Vassilopoulos [28]. FADAS predicts as well the trend of the three-stage stiffness degradation which is higher for lower stress levels although the difference is less pronounced than in the experimental data. Furthermore, the stiffness degradation predictions are lower in general than the experimental values.

Tensile and compressive residual strength tests were performed after CA cyclic loading at three stress levels, namely 372 MPa (expected $N=1000$ cycles), 252 MPa (50000 cycles) and 186 MPa ($1 \cdot 10^6$ cycles) for three life fractions, 20%, 50% or 80%, see [25]-[26]. The residual strength predictions of the $[(\pm 45/0)_4/\pm 45]_T$ laminate at $R=0.1$ were compared to the experimental data in Fig. 7.

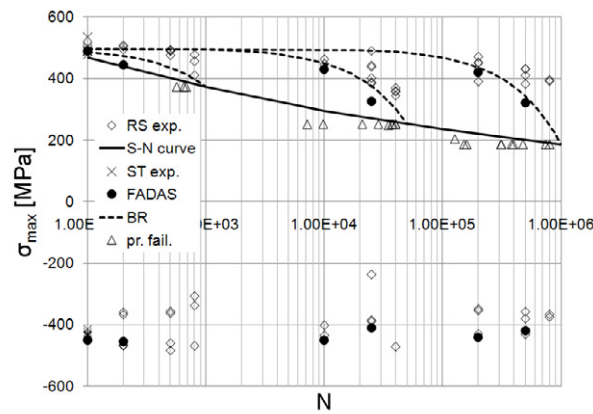


Fig. 7: Residual strength of the MD laminate after CA loading under $R=0.1$

The tensile residual strength results are in good agreement with the macroscopic BR model at the lower stress levels while they are more conservative at the higher one. The compressive residual strength predictions show insignificant strength degradation which is also the case for the tests. Similar results were also derived for other stress ratios, e.g. $R=-1$.

It is interesting to note that the residual compressive strength after tension-tension cyclic loading cannot be predicted with macroscopic models such as the sudden death described by Eq. (6) of [1] while it can be efficiently predicted with FADAS.

5.2.3. MD laminate $[(\pm 45/0)_4/\pm 45]_T$ off-axis loaded under $R=-1$

Two more data sets from CA cyclic testing of coupons cut off-axis at 10° and 60° from the $[(\pm 45/0)_4/\pm 45]_T$ laminate were reported by Philippidis et al. [22]. This test series was aiming to generate different complex stress states in the layers of the MD lay-up and investigate the effect on numerical life prediction of lay-ups without fibres in the load direction. The stacking sequence of these off-axis coupons was given by $[(55/-35/10)_4/55/-35]_T$ and $[(-75/15/60)_4/-75/15]_T$ respectively.

Tests were performed at two stress levels, high and low, under reversed loading, $R=-1$. Experimental results along with FADAS numerical predictions for both lay-ups were presented in Fig. 8. For the $[(55/-35/10)_4/55/-35]_T$ coupons, numerical simulations were performed for $\sigma_{\max}=230, 172$ and 114 MPa while $\sigma_{\max}=105, 87$ and 54 MPa were the corresponding levels for the MD [60]-off-axis coupons.

The agreement between numerical predictions and experimental data is not as good as for the previously presented S-N curves for the MD and the $[\pm 45]_S$ laminates, this time

the FADAS predictions being optimistic. Final failure was dominated in both cases by fibre fracture of the [10] or [15] plies of the 10° and 60° off-axis MD laminates while all their other plies failed very early at various matrix damage modes, see Fig. 9, 10. The reason for the disagreement observed in Fig. 8 between the FADAS predictions and the test results is attributed to the Fibre Fracture (FF) criteria implemented in Puck failure theory [29]. Indeed, these limit conditions neglect the effect of in-plane shear stress on fibre fracture under tension and in the [10], [15] plies of the above laminates significant such stresses were developed that could drastically affect the mechanisms causing fibre fracture. The adoption of different FF criteria, including the effect of in-plane shear stress could improve these results as it was suggested in [30].

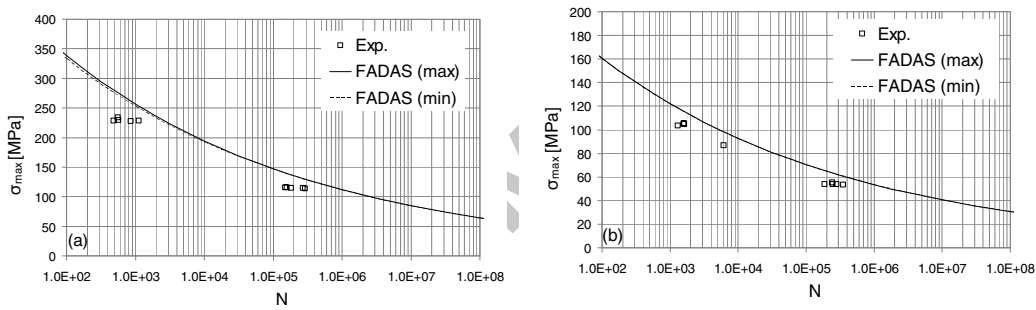


Fig. 8: Fatigue strength of off-axis loaded MD coupons under $R=-1$

(a) $[35/-55/-10]_4/35/-55]_T$, (b) $[(-75/15/60)_4/15/-75]_T$

The different colours in Fig. 9-10 correspond to different failure modes. FF_T and FF_C stand for fibre fracture in tension and compression respectively while IFF_A , IFF_B and IFF_C for inter-fibre fracture modes A, B and C respectively, see Puck and Schürmann [29].

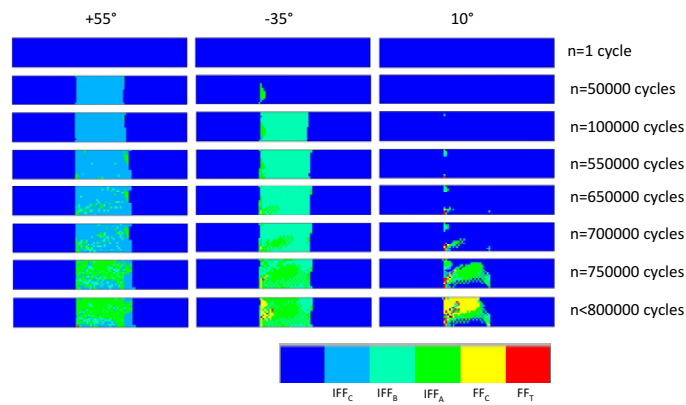


Fig. 9: Damage progression in the $[(55/-35/10)_4/55/-35]_T$ laminate. $R=-1$, $\sigma_{\max}=114$ MPa

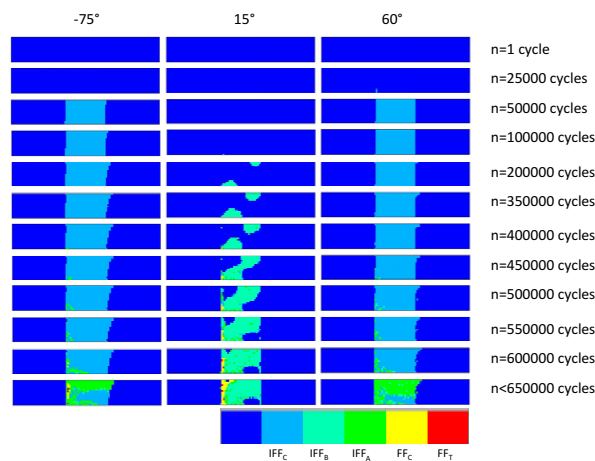


Fig. 10: Damage progression in the $[(-75/15/60)_4/-75/15]_T$ laminate. $R=-1$, $\sigma_{\max}=54$ MPa

The predicted failure modes of the $[(55/-35/10)_4/55/-35]_T$ laminate at final failure, corresponding to $n<800,000$ cycles of Fig. 9, were compared visually to a failed coupon, see Fig. 11. The outer visible [-35] ply appears to have matrix cracks at most of the gauge length area. Compressive fibre fracture can be also observed along with fibre splitting and delaminated bundles. Explosive IFF mode C in the [55] ply underneath has probably contributed to this debonding. Besides matrix cracks at the entire gauge length area of the [-35] and [55] plies, FADAS has also predicted compressive fibre fracture extending along the width of the [-35] and [10] layers. Predictions were in fair agreement with the visual observations, although a damage mode such as delamination cannot be predicted with the actual FE shell element implementation of the routine.

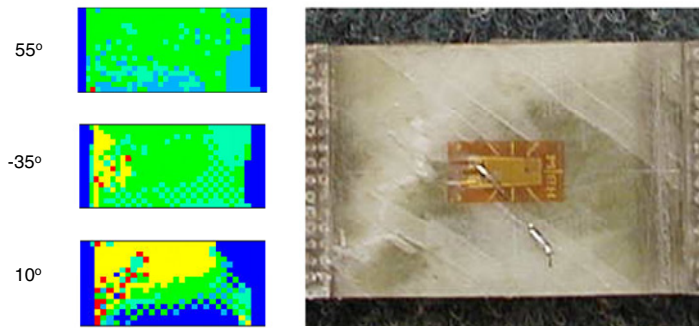


Fig. 11: Comparison of the predicted failure modes for the $[(55/-35/10)_4/55/-35]_T$

laminate with a failed coupon. $R=-1$, $\sigma_{\max}=114$ MPa

Concerning the $[(-75/15/60)_4/-75/15]_T$ coupon, see Fig. 12, FADAS predicted matrix failure at all plies and fibre fracture at the $[-75]$ and $[15]$ plies near the left tab at final failure. As it can be seen in the top surface of the failed coupon, matrix cracks spread at the entire gauge length of the outer $[-75]$ ply along with compressive fibre fracture near the left tab, validating the numerical predictions.

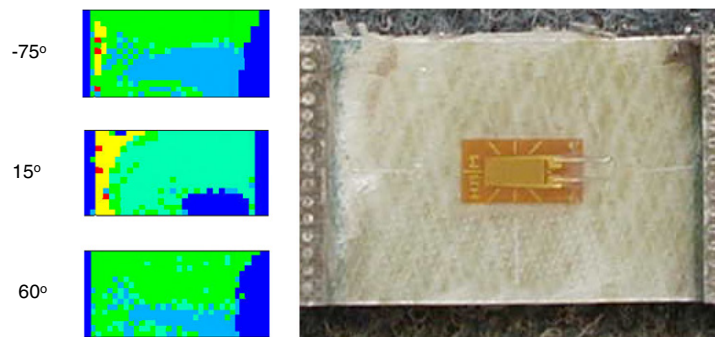


Fig. 12: Comparison of the predicted failure modes for the $[(-75/15/60)_4/-75/15]_T$

laminate with a failed coupon. $R=-1$, $\sigma_{\max}=54$ MPa

6. Conclusions

The numerical implementation of an anisotropic non-linear constitutive model with progressive damage features in a commercial FE code was presented in this paper. FADAS can be used to predict life and residual strength/stiffness of composite

laminates subjected to static or cyclic multi-axial loading. In-plane mechanical properties of the material were fully characterized at the UD ply level while fatigue strength and stiffness/strength degradation of any multidirectional stacking sequence was predicted.

The model was set up for a Glass/Epoxy UD material typical of those used in the wind turbine rotor blade industry and has been verified through a series of constant amplitude fatigue and residual strength tests on different lay-ups, simulating a variety of plane stress combinations and failure modes under various stress ratios R .

The results indicate that the actual FE implementation of the FADAS algorithm yielded satisfactory predictions for the fatigue strength under CA axial loading and also for the static residual strength of prismatic specimens. The stiffness degradation predictions, slightly lower than the experimental ones, were in agreement with the repeatedly observed experimental behaviour of the MD composite laminates, i.e. the three-stage stiffness degradation being higher for lower stress levels.

The early predicted failure initiation, even from the first cycles, highlights the importance of using damage tolerant methods, like FADAS, for realistic simulation of the mechanical behaviour of composite laminates under cyclic loading.

Acknowledgements

Research was funded in part by the European Commission in the framework of the research programme “Integrated Wind Turbine Design” (UPWIND), contract No: 019945, SES6. Partial funding was also provided by the General Secretariat of Research

and Technology (GSRT) of the Greek Ministry of Development, contract No. F.K. C037.

References

1. Eliopoulos EN, Philippidis TP, A progressive damage simulation algorithm for GFRP composites under cyclic loading. Part I: Material constitutive model, *Compos Sci Tech*, submitted for publication (2010)
2. Shokrieh MM, Lessard LB, Progressive fatigue damage modelling of composite materials, Part I: Modeling. *J Compos Mater* 2000; **34**(13), 1056-1080
3. Shokrieh MM, Lessard LB, Progressive fatigue damage modelling of composite materials, Part II: Material Characterization and model verification. *J Compos Mater* 2000; **34**(13), 1081-1116
4. Van Paepegem W, Degrieck J, Fatigue degradation modelling of plain woven glass/epoxy composites. *Compos: Part A* 2001; **32**, 1433-1441
5. Van Paepegem W, Degrieck J, De Baets P, Finite element approach for modelling fatigue damage in fibre-reinforced composite materials. *Compos: Part B* 2001; **32**, 575-588
6. Van Paepegem W, Degrieck J, A new coupled approach of residual stiffness and strength for fatigue of fibre-reinforced composites. *Int J Fatigue* 2002; **24**, 747-762
7. Van Paepegem W, Degrieck J, Coupled residual stiffness and strength model for fatigue of fibre-reinforced composite materials. *Compos Sci Tech* 2002; **62**, 687-696
8. Van Paepegem W, Degrieck J, Modelling damage and permanent strain in fibre-reinforced composites under in-plane fatigue loading. *Compos Sci Tech* 2003; **63**, 677-694
9. Van Paepegem W, Dechaene R, Degrieck J, Nonlinear correction to the bending stiffness of a damaged composite beam. *Composite Structures* 2005; **67**, 359-364

10. Gagel A, Fiedler B, Schulte K, On modelling the mechanical degradation of fatigue loaded glass-fibre non-crimp fabric reinforced epoxy laminates. *Compos Sci Tech* 2006; 66; 657-664
11. Hochard Ch, Payan J, Bordreuil C, A progressive first ply failure model for woven ply CFRP laminates under static and fatigue loads. *Int J Fatigue* 2006; 28; 1270-1276
12. Sihm S, Park JW, MAE: An Integrated Design Tool for Failure and Life Prediction of Composites, *J Compos Mater* 2008; **42**(18), 1967-1988
13. Lian W, Yao W, Fatigue life prediction of composite laminates by FEA simulation method, *Int J Fatigue* 2010; **32**(1), 123-133
14. Philippidis TP, Eliopoulos EN, A progressive damage mechanics algorithm for life prediction of composite materials under cyclic complex stress, in *Fatigue life prediction of composites and composite structures*, ed. A. P. Vassilopoulos, Woodhead Publishing Ltd and CRC Press, 2010, Chapter 11, 390-436
15. Broutman LJ, Sahu S, A new theory to predict cumulative fatigue damage in fibreglass reinforced plastics, *Composite materials: Testing and design (2nd conference)* ASTM STP 497, 1972, 170-188
16. Schaff JR, Davidson BD, Life Prediction Methodology for Composite Structures. Part II-Spectrum Fatigue, *J Compos Mater* 1997; **31**(2), 158-181
17. Eliopoulos EN, Numerical simulation of damage progression in GFRP composites under cyclic loading, 2007, Draft version of PhD thesis, University of Patras
18. Release 11.0 documentation for ANSYS, 2007 SAS IP, Inc.
19. Guide to ANSYS programmable features, ANSYS Release 6.1, 2002
20. Philippidis TP, Assimakopoulou TT, Passipoularidis VA & Antoniou AE, Static and fatigue tests on ISO standard $\pm 45^\circ$ coupons Main test phase I. OB_TG2_R020, 2004 (<http://www.wmc.eu/optimatblades.php>)

21. Krause O, Kensche C, Summary fatigue test report. OB_TG1_R026, 2006
(<http://www.wmc.eu/optimatblades.php>)
22. Philippidis TP, Antoniou AE, Assimakopoulou TT & Passipoularidis VA, Fatigue tests on OB unidirectional & multidirectional off-axis coupons Main test phase I. OB_TG2_R030, 2006 (<http://www.wmc.eu/optimatblades.php>)
23. Philippidis TP, Assimakopoulou TT, Antoniou AE, Passipoularidis VA, Residual strength tests on ISO standard $\pm 45^\circ$ coupons, OB_TG5_R008, 2005
(<http://www.wmc.eu/optimatblades.php>)
24. Philippidis TP, Assimakopoulou TT, Antoniou AE, Passipoularidis VA, Residual strength tests on ISO standard $\pm 45^\circ$ coupons, Main test phase II, OB_TG2_R037, 2006
(<http://www.wmc.eu/optimatblades.php>)
25. Nijssen R, van Wingerde A, Residual strength tests-data and analysis, OB_TG5_R007, 2006 (<http://www.wmc.eu/optimatblades.php>)
26. Dutton AG, Robertson SJ, Canfer SJ, Blanch MJ, Residual strength testing of OPTIMAT MD specimens-tests by CCLRC-RAL, OB_TG5_R012, 2006
(<http://www.wmc.eu/optimatblades.php>)
27. Nijssen RPL, Knowledge Centre WMC, Wieringerwerf, The Netherlands, personal communication 2007
28. Philippidis TP, Vassilopoulos AP, Fatigue of composite laminates under off-axis loading, Int J Fatigue 1999; **21**, 253-262
29. Puck A, Schürmann H, Failure analysis of FPF laminates by means of physically based phenomenological models, Compos Sci Tech 1998; **58**, 1045-1067
30. Antoniou AE, Kensche CW, Philippidis TP. Mechanical behaviour of glass/epoxy tubes under combined static loading. Part II: Validation of FEA progressive damage model. Compos Sci Tech 2009; **69**(13):2248–55